







ORIGINAL ARTICLE

Determination of geometric parameters of highways using classical and modern technologies

Zhuldyz Askarovna Alpyspayeva ¹, Natalya Aleksandrovna Parkhomenko ²,
Saule Kazhapovna Makenova ¹, Ewa Joanna Świerczyńska ^{3*}, Maria Elżbieta
Kowalska ³ and Janina Zaczek-Peplinska ³

¹Faculty of Land Management, architecture and design, Kazakh Agrotechnical Research University named after S. Seifullin, 62 Zhenis, 010000, Astana, Republic of Kazakhstan

²Faculty of Land Management, Omsk State Agrarian University named after P.A.Stolypin, 1 Institutskaya Ploshchad, 644008, Omsk, Russia

³Faculty of Geodesy and Cartography, Warsaw University of Technology, 1 Politechniki Square, 00-661, Warsaw, Poland

*ewa.swierczynska@pw.edu.pl

Abstract

Road upgrading to increase freight and passenger transport capacity requires surveying services, carried out at every stage of construction. During the construction of road sections designed as curves or arcs, their shape must be constantly monitored. During surveying, it is necessary to determine the elements of curves, in particular the radius and length of the curve, as well as the bisector, tangents, and angle of return of the tangents. The article presents a methodology for determining the radii of curves on highways using a GNSS system receiver with planar rectangular coordinates derived through post-processing using the Trimble Geomatics Office (TGO) software. In addition, the authors present the results of measurements of the height markers of the bottom layer of the substructure on the section from measuring point 1015+40 to measuring point 1020+00 of the Astana-Petropavlovsk highway. On the test object, tests were carried out on the technical condition of the pavement. The results were determined by the parameter. The highway section was also examined geometrically on the basis of levelling measurements. The paper proposes a methodology for road construction work that divides the measurements into two stages: initial — based on GNSS technology, and a second one — based on the levelling method.

Key words: Global Satellite Navigation Systems, geodetic surveys, transportation construction, road geometry, optimization of calculations

1 Introduction

Roadway geometric data, user behavior, and crash data provide the main input for developing existing highway safety evaluations (Cefalo et al., 2017). Traffic safety and potential risk management are crucial to achieving a safe, balanced, and sustainable road transport system. To enhance the quality of transport infrastructure, comprehensive studies are necessary, with particular focus on the design,

construction, and operation stages. This has led to the concept of creating a "passport" for transport facilities, which would cover the entire life cycle of the given piece of infrastructure (Shutin and Dolgov, 2019). The fundamental data for the Digital Passport of a transport object are geometric data. Easy, effective, and reliable methods for obtaining this type of data are crucial in monitoring extensive such linear structures as roads.

Numerous scientific studies explore various platforms like UAVs

(unmanned aerial vehicles), ground robots, smartphones, and ground vehicles equipped with modern measurement technologies such as GNSS (Global Navigation Satellite Systems), LiDAR (Light Detection and Ranging) and other sensors to assess the condition and geometry of roads (Bazhenov, 2021; Di Graziano et al., 2020; Ranyal et al., 2022). Traditional methods for obtaining geometric data include: theodolites, total stations, spirit levels, rods, measuring tapes, rulers, sights, as well as various templates and mechanical devices. However, technological advancements now allow for significantly faster measurement methods, often using units pre-installed on moving devices. Remote-sensing technologies for road information inventory are rapidly developing (Guan et al., 2016), offering the possibility of acquiring three-dimensional (3D) information on large-area roadways with survey-grade accuracy at traffic speeds, thus providing new and efficient ways for the road information inventory.

The adoption of modern measurement techniques requires the development of appropriate methodologies for data acquisition and processing as well as their application in field conditions. The coordinate method is currently a default in setting out curves in the field, where coordinates of points calculated using formulas are imported into instruments via dedicated software. In road construction, surveying work begins with route preparation, which involves reconnaissance activities to designate control points and outline the equipment's movement route. This process includes establishing a reference geodetic network using temporary anchor points, with baselines subdivided at the start and end of the mobile laboratory's movement. Temporary points are linked to continuously-operational base stations through static observations or PPP (Precise Point Positioning), ensuring measurement consistency and adherence to the WGS-84 or GSK-2011 coordinate system (State Geodetic Coordinate System).

During measurements, it is necessary to determine the geometric parameters of curves, particularly the radius and length of curvature, bisector, tangents, and angle of rotation. Various methods can be employed to address this task. Before detailing the layout of the arc on-site, the positions of the turning angle apex, the beginning, the middle, and the end of the arc are determined. The spacing between points along the curve is determined by the curve's length, radius, and construction method. Determining curve radii is a crucial aspect of comprehensive geodetic control in road construction. The geodetic control procedures employed in highway construction include the following operations: route reconstruction, control during roadbed construction, layout of artificial structure axes, detailed layout of circular and transitional curves, plan-altitude control during pavement laying, and executive surveying. The aim of this work was to explore the capabilities of satellite positioning systems in assessing the technical condition of roads. Its main focus was on determining the geometric parameters of vertical arches.

GNSS are actively used to address diverse industrial and geospatial challenges (Boyarchuk et al., 2022; Catania et al., 2020; Lobatskaya and Strelchenko, 2016; Pomortseva et al., 2020; Prokhorov and Medvedev, 2022; Vatseva et al., 2013). The utilization of contemporary GNSS receivers for real-time data acquisition in geodetic surveying on highways has been extensively discussed in literature (Gorda, 2020; Hryhorovskiy et al., 2020; Karan et al., 2014; Tikhomirov et al., 2022). Compared to traditional geodetic technologies, these systems offer additional advantages, including:

- a broad range of accuracies in determining the location of objects, spanning from tens of meters to millimeters,
- high labor productivity attributed to the rapid acquisition of information (5 to 10 times faster than classical technologies),
- economic efficiency, as there is no need for direct visibility between geodetic points and the transmission of complex signals,
- independence from weather conditions,
- high process automation,
- the capability to conduct observations in kinematics, and more.

Satellite technologies also present specific limitations, such as susceptibility to obstacles in close proximity to the satellite antenna (elevation mask), the need for intricate coordinate transformations between different systems, including the complexities associated with obtaining orthometric heights, and other challenges.

World-wide most execution work has been replaced by construction equipment. The work of excavators and graders is controlled by a suitable system using positioning methods: RTK-GNSS and Total Station. Machine control is being implemented on construction sites (Raza et al., 2022). The role of the surveyor is primarily to generate 3D models of the project, which are uploaded into the system that controls the work of machines in real time, with the advantage of reducing the risk of execution errors, as well as minimizing staking and inspection work.

However, solutions based on GNSS or Total Station positioning are expensive and unavailable in some countries. Like laser scanning, BIM (Han et al., 2023) or UAV technology (Han et al., 2021), machine control technology for excavators or graders requires modern equipment that contractors in many countries cannot afford. The article is an attempt to modernize and update traditional methods, which are still used for economic reasons.

The paper proposes a methodology for road construction work that divides control measurements into two stages. In the first stage, which consists of earthworks and construction of initial layers, GNSS satellite technology is used. This method allows a horizontal accuracy of 1–3 cm and an elevation accuracy of 1–5 cm. In the second stage, which involves the construction of subsequent road layers, levelling technology is used. Successively, as the work progresses, the accuracy of control measurements must be increased, and levelling provides an elevation accuracy of 1 cm.

Another goal of this research was to develop algorithms for the automatic detection of deviations of curve heights from nominal values, based on geometric and statistical laws. This article is organized as follows: the Methods section presents the geometric relationships between the parameters of the vertical curve and outlines the procedure of the conducted research along with the theoretical aspects of the statistical analyses. The Research Results section presents the values obtained. The Discussion section compares the methods used and their reflection in existing studies using similar technologies. Finally, the Conclusion section provides a summary and concluding remarks.

2 Methods

Let us initially examine a well-established geometric theorem and present its proof in the context of road geometry. This theorem concerns the central angle of a circle and the angle inscribed in a circle, both based on the same arc of the circle. Subsequently, methods for determining the radii and elements of circular curves will be developed based on this theorem. The content of the theorem and its proof are illustrated in Figure 1.

Theorem: the central angle formed by radii and resting on the arc of the circle (2-3) is equal to twice the inscribed angle b , which is formed by segments (1-2 and 1-3). This angle can be drawn to the given arc from any point on the circle that does not lie on the arc. The proof is provided below:

Proof: let us consider the isosceles triangles 0-1-2 and 0-1-3 (Figure 1). From triangle 0-1-2, we have:

$$\gamma = 180^\circ - x - b - x - b = 180^\circ - 2x - 2b \quad (1)$$

From triangle 0-1-3, we have:

$$\gamma = 180^\circ - x - b - x - b = 180^\circ - 2x - 2b \quad (2)$$

where: γ – the central angle formed by radii and resting on the arc of the circle (1-2); z – the central angle formed by radii and resting

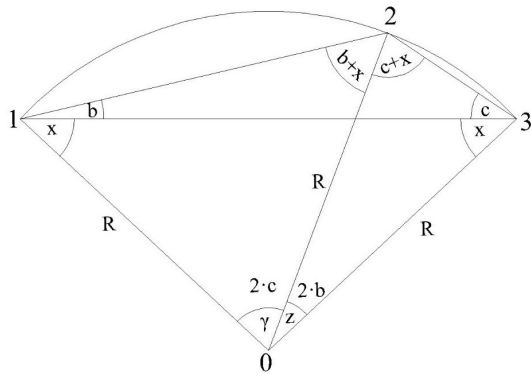


Figure 1. Diagram illustrating the relationship between the central angle z and the inscribed angle b

on the arc of the circle (2-3); b – the angle inscribed in the circle and resting on the arc of the circle (2-3); x – the angle inscribed in the circle between the radius and the bisector of the arc of the circle (1-3).

When point 1 is displaced to another part of the circle, with the position of the circle arc (2-3) remaining unchanged, the relationship $z = 2b$ is maintained.

The presented theorem serves as the foundation for methods aimed at determining the radii of circular curves during the passportization and reconstruction of roads, utilizing satellite navigation system receivers and electronic tachymeters. In the passportization of highways, particularly in areas where straight sections are relatively short or practically non-existent, such as when using splines for tracing, the determination of curve parameters requires establishing the coordinates of at least three points, as depicted in Figure 2.

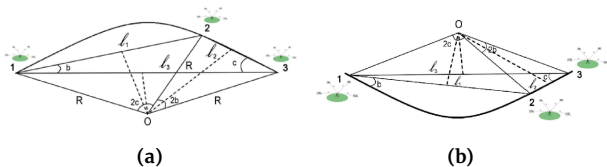


Figure 2. (a) – determination of curve radii using three points. The following adjustments have been made to the text: 1,2,3 – points of GNSS receiver installation for coordinate determination; l_1, l_2, l_3 – chords connecting the locations of points; R – radius of the circular curve; (b) – a concave curve is depicted

The sequence of actions for determining the geometric parameters of highways using GNSS receivers is illustrated in Figure 3. The methodology presented in this chapter involves the use of geodetic-class GNSS receivers – planned within the range of 0.5 cm to 3 cm. The coordinates are initially determined in the WGS-84 system and subsequently transformed into rectangular coordinates using such software as: LGO, TBC, and Topcon Tools. For measurement control, it is imperative to solve the inverse geodetic problem within a designated software module to obtain the relevant angles and line lengths. Figure 3 shows the scheme for determining the radius in the vertical plane. The calculations involve finding angles b and c . Using these angles and chord lengths, the radius and length of the curve can be calculated.

By solving inverse geodetic problems, the intermediate parameters of the survey structure are determined according to the formulas:

$$\tan v = \frac{h}{d}; \quad l = \sqrt{d^2 + h^2} \quad (3)$$

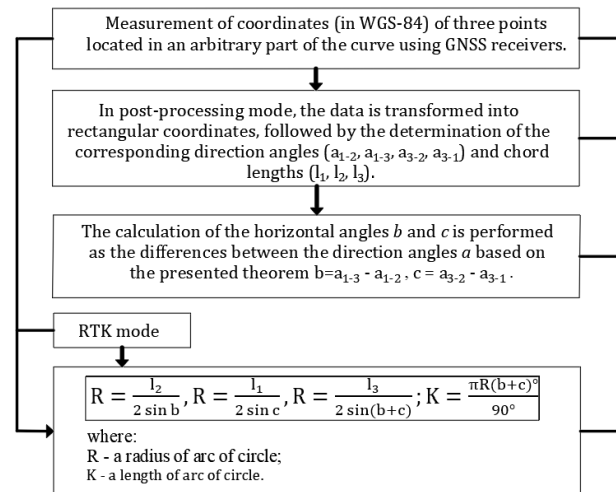


Figure 3. Algorithm of production actions

where: h – the vertical distance between two points, representing the difference in height; d – the horizontal distance between two points, calculated as the square root of the sum of the squares of the differences between the horizontal coordinates; v – the vertical angles, from which the angles inscribed in the circle and based on arcs (2-3) and (1-2), respectively, are calculated:

$$b = v_{1-2} - v_{1-3}; \quad c = v_{3-1} - v_{3-2} \quad (4)$$

Based on the formulas illustrated in Figure 4, the root mean square error (RMS) in the determination of radius and RMS of the length of the curve will be equal to:

$$m_R = \sqrt{m_1^2 \left(\frac{1}{2 \sin(b)} \right)^2 + m_b^2 \left(\frac{\cos(b)l}{2\rho \sin^2(b)} \right)^2} \quad (5)$$

$$m_K = \sqrt{m_R^2 (0.035\beta)^2 + m_\beta^2 \left(\frac{0.035R}{\rho\beta} \right)^2}$$

where: m_R – RMS of radius determination; m_1 – RMS of chord length determination (positioning accuracy by geodetic-class GNSS receivers – planned within the range of 0.5 to 3 cm); m_b – RMS of determination of horizontal angles (5-10); $\rho = 206265''$; m_K – RMS of determination of the curve length; m_β – RMS of determination (measurement) of vertical angles; β – value of vertical angles, $\beta = b + c$.

In accordance with regulatory guidelines, the accuracy in determining the radii of horizontal and vertical curves on highways should be within $\pm 10\%$ of the radius R . Upon calculating the accuracy of radius determination across a range from 100 m to 3000 m for different road categories, it has been noted that the root mean square errors are consistently within the range of 0.1 m to 1 m. This level of precision significantly surpasses the recommended requirements.

In addition to the coordinate method, an alternative approach employs an electronic theodolite, wherein chord lengths (l) and angles (b, c) are not computed, but, instead, are measured directly in the field, as depicted in Figure 4. This method of control proves particularly effective in highway construction (Bazhenov, 2021).

By designating K (20, 50, 100 m) as a constant in formula $R = \frac{K90^\circ}{\pi b^\circ}$, a direct dependency of the radius on the horizontal angle b is established. For fixed values of the arc length, the formula uses the following expressions: when $K_f = 20$ then $R = \frac{573.248}{b}$; when $K_f = 50$ then $R = \frac{1433.121}{b}$; when $K_f = 100$ then $R = \frac{2866.242}{b}$. The developed method facilitates a rapid determination of radii in circu-

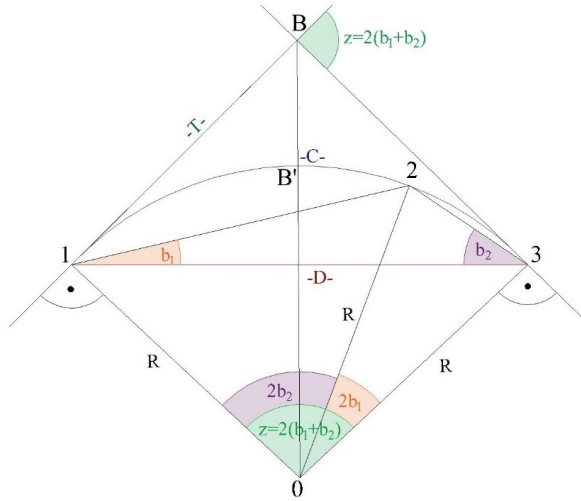


Figure 4. Method of real-time determination of radii in a circular curve

lar curves on highways following the measurement of the angle b . This involves positioning an electronic theodolite at any point along the curve, either preceding the laid arc of fixed length or beyond it and subsequently measuring the angle at the ends of the arc. For practical implementation in production settings, specialized tables can be devised. These tables allow for the direct determination of the radius value based on the angle b values calculated at specific intervals. When it is necessary to determine not only the radius but also the other elements of the curve (curve, tangent, bisector), a fixed arc length K_f (the end of the curve-1) should be laid out from points at the beginning or end of the curve. Angles b_1 (the angle inscribed in the circle and resting on the arc of circle 2-3) and b_2 (the angle inscribed in the circle and resting on the arc of circle 1-2) should be measured accordingly from these points.

Then, the elements of the curve will be determined from the following relationships:

$$\begin{aligned} T &= R \tan(b_1 + b_2) \\ C &= \frac{\pi R^2(b_1 + b_2)}{180^\circ} = \frac{\pi R(b_1 + b_2)}{90^\circ} \\ B &= R (\sec(b_1 + b_2) - 1) \end{aligned} \quad (6)$$

where: T – the length of the tangent to the arc of the circle, $T = |1B| = |B3|$; C – the arc length of the circle; B – the distance between the vertex of the arc of a circle and the center of the arc of the circle, $B = |BB'|$.

The method for determining curve parameters described above is recommended when there is direct visibility between the points at the beginning and the end of the curve. The accuracy of radius determination, denoted as m_R , will depend on the precision of measuring angles β and radius lengths R , and can be calculated using the following formula: $m_R = m_\beta R$. In the measurements taken with the Sokkia 530RL electronic theodolite, which has an angular accuracy of 5", the root mean square error in radius determination will be as follows: for radii up to 500 m $m_R = 0.01$ m, for radii up to 1000 m $m_R = 0.02$ m, for radii up to 5000 m $m_R = 0.12$ m.

3 Results

Table 1 presents a comparative analysis of techniques employed in ascertaining geometric parameters in highway construction and inventorying. The method described is both applicable and implementable in the Real-Time Kinematic (RTK) mode. In this scenario, rectangular coordinates are determined on-site in real time, allow-

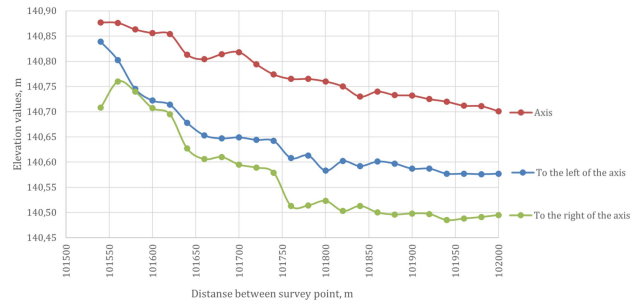


Figure 5. Results of the executive survey of survey points from the bottom layer of the base on the section from survey point 1015+40 to survey point 1020+00 of the "Astana-Petropavlovsk" highway. Elevation changes along the investigated section of the highway.

ing for rapid calculations of geometric parameters.

To analyze the quality of the highway, we used data from the executive survey at the reconstruction site of the "Astana-Petropavlovsk" highway, part of the transit corridor "Borovoye-Kokshetau-Petropavlovsk-Russian Federation border" (km 418–443). At that time, the existing road corresponded to technical category III, and it was being upgraded to meet the technical category II standards. The road surface levelling survey was carried out based on height marks of the top of the bottom layer of the road base from PK 1015+40 to PK 1020+00, covering a length of 460 meters. The levelling was conducted using Sokkia C330 levellers and telescopic 5-meter laths every 20 meters along the route's axis and the edges of the roadway. Based on the elevation values of the road axis and right and left edges, a graph was created to clearly show the difference in elevations and the curvature of the roadbed (Figure 5).

The study of the levelness of the highway was carried out by calculating the amplitude differences of elevations according to formula:

$$\delta h_i = \left| \frac{h_{i-k} + h_{i+k}}{2} - h_i \pm \Delta_i \right| \quad (7)$$

where: h_i – is the relative elevation of the point for which the deviation is determined; h_{i-k} and h_{i+k} – are relative marks of the preceding and following points, respectively; i – number of the point for which the deviation is determined; $i - k$ and $i + k$ – ordinal numbers of the previous and subsequent points, respectively; Δ_i – correction for the radius of the vertical curve.

The subject of the study is assigned a longitudinal micro profile in the form of an array of ordinates (amplitudes), allowing for the distance between the fixed ordinates to be a few centimeters. The accuracy of their measurement increases to millimeter values, depending on the capabilities of the applied equipment.

The values obtained from the calculation are presented in Figure 6. In accordance with GOST R 5926–2016 (Scalco et al., 2023) and GOST 33101–2014 (Butenko and Nevoit, 2021), the total number of δh_i values obtained should be taken as 100%, and the number of δh_i values less than those established by SP 78.13330 should be calculated with an accuracy of 0.1%. According to SP 78.13330.2012 (Kovrov, 2022), 90% of the determinations should be within the limits of 24 mm, and 10% of determinations should not exceed these values by more than 1.5 times.

When analyzing the compliance with the established requirements for the levelness of a highway of technical category III, to which the investigated road section of the "Astana-Petropavlovsk" highway belongs, all received amplitudes were converted to absolute values to calculate the percentage ratio of acceptable and unacceptable values.

Table 1. Techniques for determining geometric parameters on highways (Nikitin, 2018; Katkalo, 2012)

Methods	Normative	Mechanized	Katkalo Yu.A.	Nikitin A.V.
Indicators				
Construction Control	Constrained by local conditions	Difficult to execute	Difficulties in mountainous conditions	Effective (determines horizontal and vertical radii of curves)
Verification of Geometric Parameters during Inventorying	Requires significant time investment	Accuracy is determined by the conditions of the road surface and the inertial system	Difficulty in selecting the theodolite position	Independent of the terrain and conditions beyond the road surface
Degree of agreement	Low (due to the ambiguity in determining turning angles and tangents)	High (assuming a quality upper layer of road pavement)	Complies with regulatory requirements	High (determined by the accuracy of modern GNSS receivers)

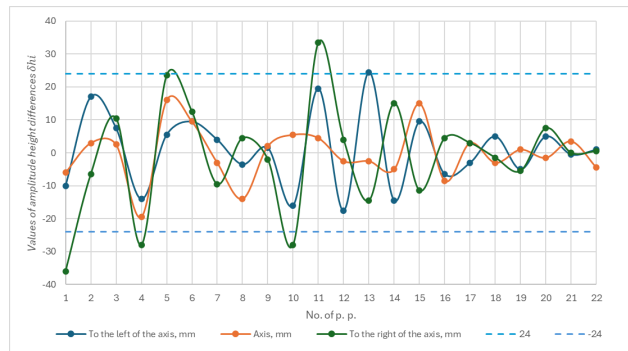


Figure 6. Calculated amplitude height differences Δh_i on the section of the "Astana-Petropavlovsk" highway

Table 2. International Roughness Index condition rating scale for sealed roads

Pavement condition	perfectly	good	satisfactorily	unsatisfactorily
International Roughness Index (IRI)	< 2.50	2.50 – 3.00	3.00 – 3.40	> 3.40

On the road axis, all amplitude differences did not exceed the permissible value of 24 mm, which means that the central part of the road surface can be considered flat. On the left part of the axis, there is a deviation exceeding the limit value, but more than 95% of all 22 amplitudes are within the limit set by the normative documentation, and the remaining value does not exceed the specified tolerance more than 1.5 times (24.5 mm does not exceed the value 24 mm*1.5 = 36 mm). On the right side of the road, 20% of determinations do not meet the tolerance of 24 mm, but they do not exceed 36 mm.

Thus, the deviations obtained on the axis and on the left edge of the road fully comply with the required levelness for a category II highway. However, on the right edge, according to the normative documentation, the values for four amplitude differences (points 1, 4, 10, 11) along the investigated section of the route (Figure 6) are beyond the tolerated range. Since this layer of the roadbed is the bottom layer, it is necessary to lay the subsequent layer taking into account the unevenness in places with unacceptable values.

In addition to assessing the geometric properties of the highway of the base and pavement layers by determining the algebraic differences in elevations (amplitudes), the flatness of the roadway should be verified using the International Roughness Index (IRI) (Cruz et al., 2021; Golov et al., 2022; Múčka, 2017)(see Table 2).

Relative elevations were determined by profilometer, and eleva-

Table 3. Relative elevations, determined using a profilometer, showing the height differences between two points that are 250 mm apart

km	IRI readings, m/km		average value, m/km	IRI index score
	forward direction	reverse direction		
1	2	3	4	5
46+200	4.24	2.21	3.23	satisfactorily
46+300	3.72	1.72	2.72	good
46+400	3.80	2.12	2.96	good
46+500	2.59	1.42	2.01	perfectly
46+600	3.02	2.57	2.80	good
46+700	3.46	2.44	2.95	good
46+800	3.18	2.21	2.70	good
46+900	2.28	1.72	2.00	perfectly
47+000	4.02	2.12	3.07	good
47+100	3.61	1.42	2.52	perfectly
47+200	2.94	2.57	2.76	good
47+300	2.80	2.44	2.62	good
47+400	3.21	2.58	2.90	good
47+500	4.35	1.99	3.17	satisfactorily
47+600	2.58	2.03	2.31	perfectly
47+700	2.44	2.08	2.26	perfectly
47+800	3.08	2.34	2.71	good
47+900	3.76	2.01	2.89	good
48+000	2.78	2.53	2.66	good
48+100	2.39	1.70	2.05	perfectly
48+200	2.23	1.84	2.04	perfectly
48+300	2.56	1.79	2.18	perfectly
48+400	3.22	1.86	2.54	perfectly
48+500	4.63	1.63	3.13	satisfactorily
48+600	4.74	2.09	3.42	unsatisfactorily
48+700	4.47	2.53	3.50	unsatisfactorily

tion differences were calculated between two points with an interval of 250 mm. The measurement data obtained are presented in Table 3 and in a graph in Figure 7. The last column of Table 3 shows the IRI values. The research has shown that more than 59% of the surveyed section is in a good condition, and the section requiring repair account for more than 30% of the total length.

Since during construction on the investigated section of the highway the acceptable values were not achieved on the right edge, it was decided to perform mathematical processing of statistical studies of road surface flatness.

In order to calculate the accuracy of laying the bottom layer of the pavement of the investigated section of the "Astana-Petropavlovsk" highway, while ensuring the permissible deviations of height marks for bases and pavements of category II public roads, it is necessary

Table 4. Statistical analysis of the results of the investigated section of the Astana-Petropavlovsk highway

Name of calculated value	Calculation results		
	Along the highway axis	Along the left edge from the highway axis	Along the right edge from the highway axis
Maximum amplitude value	$x_{\max} = 16.0 \text{ mm}$	$x_{\max} = 24.5 \text{ mm}$	$x_{\max} = 33.5 \text{ mm}$
Minimum amplitude value	$x_{\min} = -19.5 \text{ mm}$	$x_{\min} = -17.5 \text{ mm}$	$x_{\min} = -36.0 \text{ mm}$
Range of variation	$R = 16 - (-19.5) = 35.5 \text{ mm}$	$R = 24.5 - (-17.5) = 42.0 \text{ mm}$	$R = 33.5 - (-36) = 69.5 \text{ mm}$
Interval difference	$h = 35.5 / (1 + 3.32 \cdot \lg(22))$ $h = 6.51 \text{ mm}$	$h = 42.0 / (1 + 3.32 \cdot \lg(22))$ $h = 7.70 \text{ mm}$	$h = 69.5 / (1 + 3.32 \cdot \lg(22))$ $h = 12.74 \text{ mm}$
The arithmetic mean of a series	$\bar{x} = 0.37 / 22 = 0.02 \text{ mm}$	$\bar{x} = 7.53 / 22 = 0.34 \text{ mm}$	$\bar{x} = -15.09 / 22 = -0.69 \text{ mm}$
RMS determination of amplitude differences	$m = \sqrt{740.65 / (22 - 1)}$ $m = 5.94 \text{ mm}$	$m = \sqrt{1201.94 / (22 - 1)}$ $m = 8.95 \text{ mm}$	$m = \sqrt{2889.01 / (22 - 1)}$ $m = 15.52 \text{ mm}$
RMS of the arithmetic mean	$M = 5.94 / \sqrt{22} = 1.27 \text{ mm}$	$M = 8.95 / \sqrt{22} = 1.27 \text{ mm}$	$M = 15.52 / \sqrt{22} = 3.31 \text{ mm}$
Dispersion	$D = 1417.81 / 22 = 64.45 \text{ mm}^2$	$D = 2563.48 / 22 = 116.52 \text{ mm}^2$	$D = 5898.67 / 22 = 268.12 \text{ mm}^2$
Standard deviation	$\sigma = \sqrt{64.45} = 8.03 \text{ mm}$	$\sigma = \sqrt{116.52} = 10.79 \text{ mm}$	$\sigma = \sqrt{268.12} = 16.37 \text{ mm}$
Sum of theoretical probabilities	$\Sigma P(x_i) = 0.999$	$\Sigma P(x_i) = 0.98$	$\Sigma P(x_i) = 0.98$
Confidence interval for the mathematical expectation	$-2.61 < \bar{x} < 2.64$	$-3.62 < \bar{x} < 4.30$	$-7.55 < \bar{x} < 6.18$
Confidence interval for the standard	$3.84 < \sigma < 8.04$	$5.82 < \sigma < 12.08$	$10.09 < \sigma < 20.95$

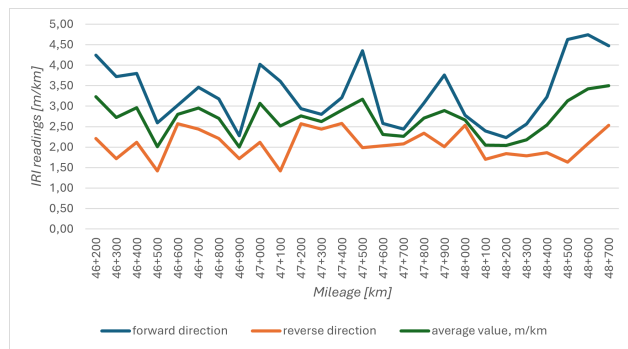


Figure 7. IRI values

to set the confidence probability $P = 0.95$ and analyze the amplitude differences of height marks under normal distribution. Therefore, it is required to establish the regularity of distribution of amplitude differences of heights by intervals (h) using the range of variation of amplitude differences of heights (R) and their number (N), taking into account the difference of their maximum and minimum values, according to the formula: $h = \frac{R}{1 + 3.32 \lg N}$. Indicators of further calculations are summarized in Table 4.

The study results show that the standard values for amplitude differences fall within the calculated confidence intervals, indicating the accuracy and reliability of the analysis performed. The analysis results led to the construction of curves showing the theoretical and practical distribution of amplitude differences of height marks along the axis, right edge, and left edge of the "Astana-Petropavlovsk" highway. These curves visually indicate that the amplitude differences in heights follow a normal distribution. To ensure the quality of the research, the results were verified with a statistical hypothesis using Pearson's χ^2 criterion. The statistical analysis of the differences in pavement height amplitudes along the road axis is presented in Table 5.

The study shows that the values of Pearson's criterion on the axis, to the left of the axis, and to the right of the axis are 2.67, 5.97, and 5.33, respectively. These values need to be compared with the

acceptable tabular value, which depends on the degrees of freedom (r) and confidence probability ($P = 95$).

With the degrees of freedom $r = 2$, the tabular value of Pearson's criterion χ^2 is 5.991. Since none of the three values exceeds the permissible value, they satisfy the given inequality, confirming the statistical hypothesis. This means the test was successful, and the amplitude differences fit the normal distribution, demonstrating the accuracy and reliability of the analysis. To ensure the functionality of mobile laser scanning systems on road surface, control points were marked on the asphalt pavement. The coordinates and heights of these points were determined in a fast static mode using temporary fixation points.

The analysis of the method for determining highway levelness through amplitude differences, using data from the executive survey with a leveler, indicates that the amplitude differences did not exceed the permissible value of 24 mm for the technical category II highway. This means that the levelness of the road corresponded to the selected design category of the public road. Furthermore, statistical processing of the obtained amplitudes showed that the measurement errors fit the normal distribution, validating the correct performance of the analysis, the accuracy of construction works, and the quality of geodetic works for controlling the highway's straightness.

The alignment of design marks was carried out at picket points of the road in the central part of the motorway and at the edges of the carriageway. Since the roadbed has several layers, the design points were taken after each paving layer. The requirements to the surveying of elevations were met with a maximum error of 10mm. As practice has shown, with the help of a GPS receiver with the use of 'real-time kinematics' technology it is possible to carry out operational surveying works with high accuracy in small areas or on objects that do not require special accuracy. It is incorrect to carry out GNSS surveying with GNSS equipment, as the equipment does not allow to maintain the required accuracy of height marking. The minimum error of determining the height coordinates of satellite equipment exceeds the required value of 10 mm.

Therefore, electronic total stations are widely used in the construction of motorways, they are built in. The programme explains how to determine the metaposition of elevation marks of the points

Table 5. Statistical processing of amplitude height differences of road surface along the axis of the "Astana-Petropavlovsk" highway; section from survey point 1015+40 to survey point 1020+00

height differences	Start of the interval a	End of the interval b	n_i	W_i	x_i	$n_i x_i$	$x_i - \bar{x}$	$n_i(x_i - \bar{x})^2$	t_1	t_2	$1/2F(t_1)$	$1/2F(t_2)$	$P(x_i)$
along the axis	-19.50	-12.99	2	0.09	-16.25	-32.49	-16.26	529.03	-3.29	-2.19	-0.50	-0.49	0.01
	-12.99	-6.49	1	0.05	-9.74	-9.74	-9.76	95.23	-2.19	-1.10	-0.49	-0.36	0.12
	-6.49	0.02	8	0.36	-3.24	-25.89	-3.25	84.65	-1.10	0.00	-0.36	0.00	0.36
	0.02	6.52	8	0.36	3.27	26.16	3.25	84.65	0.00	1.10	0.00	0.36	0.36
	6.52	13.03	1	0.05	9.78	9.78	9.76	95.23	1.10	2.19	0.36	0.49	0.12
	13.03	19.53	2	0.09	16.28	32.56	16.26	529.03	2.19	3.29	0.49	0.50	0.01
	Summations		22	1					1417.81				
along the left side of the axis	-17.50	-9.80	5	0.23	-13.65	-68.26	-13.99	979.17	-1.99	-1.13	-0.48	-0.37	0.11
	-9.80	-2.11	4	0.18	-5.95	-23.82	-6.30	158.63	-1.13	-0.27	-0.37	-0.11	0.26
	-2.11	5.59	7	0.32	1.74	12.19	1.40	13.71	-0.27	0.59	-0.11	0.22	0.33
	5.59	13.29	3	0.14	9.44	28.32	9.10	248.22	0.59	1.45	0.22	0.43	0.20
	13.29	20.98	2	0.09	17.14	34.27	16.79	564.00	1.45	2.31	0.43	0.49	0.06
	20.98	28.68	1	0.05	24.83	24.83	24.49	599.74	2.31	3.17	0.49	0.48	0.01
Summations		22	1					2563.48					0.98
along the right side of the axis	-36.00	-23.26	3	0.14	-29.63	-88.90	-28.95	2513.64	-2.28	-1.46	-0.49	-0.43	0.06
	-23.26	-10.53	2	0.09	-16.90	-33.79	-16.21	525.52	-1.46	-0.63	-0.43	-0.24	0.19
	-10.53	2.21	7	0.32	-4.16	-29.11	-3.47	84.46	-0.63	0.19	-0.24	0.08	0.31
	2.21	14.95	7	0.32	8.58	60.04	9.26	600.59	0.19	1.01	0.08	0.34	0.27
	14.95	27.68	2	0.09	21.31	42.63	22.00	967.92	1.01	1.83	0.34	0.47	0.12
	27.68	40.42	1	0.05	34.05	34.05	34.74	1206.55	1.83	2.65	0.47	0.49	0.02
Summations		22	1					5898.67					0.98

to be removed. The capabilities of the device meet the requirements of accuracy in height, and special software allows you to enter the coordinates of points for further partitioning.

4 Discussion

The developed methods for determining the geometric parameters of highways and artificial structures enable prompt and precise the execution of geodetic measurements (Bárta et al., 2021; Blachowski et al., 2014; Boyarchuk et al., 2022; Braun and Štroner, 2014; Cignetti et al., 2019; Elnabwy et al., 2013; Kovrov, 2022; Kuzmin, 2019; Mill et al., 2015; Muñoz-Salinas et al., 2009; Samsonov and Baryakh, 2020; Taşçi, 2015). This enhancement in labor productivity is achieved through a reduction in the time required for task completion. These techniques for determining curve radii have been effectively applied to ascertain the geometric parameters of adjacent roads during engineering and geodetic surveys.

Geospatial data most often obtained to control geometric parameters of motorways with geodetic measuring instruments: mobile laser scanning laboratory, electronic levellers and total stations, global navigation satellite systems (GNSS) receivers.

Certain total stations feature specialized built-in software for curve layout, typically employing circular curves. GNSS receivers also incorporate technologies for curve layout. The predominant method for staking out curves on the terrain is the coordinate approach, where point coordinates, determined through calculation formulas, are imported into the instruments using dedicated software. However, the procedural sequence for executing such tasks is currently absent from literature and manuals on geodetic instrument operation. Consequently, there is a need to adapt modern geodetic technologies to the context of road construction.

The primary focus in implementing the transportation segment of the plan is the innovative transformation of the infrastructure

construction sector. This involves the introduction and extensive adoption of advanced digital technologies.

Currently, digital technologies in transportation infrastructure represent fragmented components of various systems. There is an imperative need for a paradigm shift in the conceptualization of roads and their constituent elements. This transformation should extend to all facets of roads, encompassing design, construction supervision, and maintenance of highways.

5 Conclusion

Based on the analysis of data and the conclusions drawn, it is evident that the proposed method for determining curve radii on highways is more productive and efficient than the classical solutions. Its application ensures the precise determination of geometric parameters in the construction and operation of highways. In this paper, we have delineated the fundamental principles for curve layout, presenting geodetic methods for the layout of circular and transition curves and the control of earthwork. The paper also presents a sequence of actions for determining the geometric parameters of highways. The creation of a digital road passport is essential to address current challenges in automating road management processes and traffic flow control, including safety and information security (Boyarchuk et al., 2022; Shutin and Dolgov, 2019; Taşçi, 2015). The basis for creating a road passport, which can be used for such tasks as: road renovation, road management, and precise road navigation is the acquisition of accurate geometric data. A digital road passport can facilitate the automation of road facility management processes and enhance transportation logistics, thereby significantly increasing mobility by improving the speed of traffic flow. This advancement will promote the use of highly automated freight delivery vehicles and create conditions for the potential realization of unmanned vehicle movement.

References

- Bárta, L., Bureš, J., and Švábenský, O. (2021). Geodetic monitoring of bridge structures in operation. In *Contributions to International Conferences on Engineering Surveying: 8th INGEN International Conference on Engineering Surveying and 4th SIG Symposium on Engineering Geodesy*, pages 198–210. Springer, doi:10.1007/978-3-030-51953-7_17.
- Bazhenov, A. (2021). Information technologies in road construction. *BIM Modelling Construction And Architecture Problems*, pages 72–76, doi:10.23968/BIMAC.2021.008. (original in Russian).
- Blachowski, J., Milczarek, W., and Stefaniak, P. (2014). Deformation information system for facilitating studies of mining-ground deformations, development, and applications. *Natural Hazards and Earth System Sciences*, 14(7):1677–1689, doi:10.5194/nhess-14-1677-2014.
- Boyarchuk, M., Zhurkin, I., Nepoklonov, V., and Orlov, P. Y. (2022). Geoinformational technologies analysis for studying the visualization of the Earth's surface vertical and horizontal deformations. *Geodesy and Cartography (Lithuania)*, 988(10):53–61, doi:10.22389/0016-7126-2022-988-10-53-61.
- Braun, J. and Štroner, M. (2014). Geodetic measurement of longitudinal displacements of the railway bridge. *Geoinformatics FCE CTU*, 12:16–21, doi:10.14311/gi.12.3.
- Butenko, E. and Nevoit, N. (2021). Peculiarities of geodesic works with the use of UAVs for the needs of land management. *Zemleustrij, kadastr i monitoring zemel'*, (1), doi:10.31548/zemleustrij2021.01.08.
- Catania, P., Comparetti, A., Febo, P., Morello, G., Orlando, S., Roma, E., and Vallone, M. (2020). Positioning accuracy comparison of GNSS receivers used for mapping and guidance of agricultural machines. *Agronomy*, 10(7):924, doi:10.3390/agronomy10070924.
- Cefalo, R., Grandi, G., Roberti, R., and Sluga, T. (2017). Extraction of road geometric parameters from high resolution remote sensing images validated by GNSS/INS geodetic techniques. In *Computational Science and Its Applications—ICCSA 2017: 17th International Conference, Trieste, Italy, July 3–6, 2017, Proceedings, Part IV 17*, pages 181–195. Springer, doi:10.1007/978-3-319-62401-3_14.
- Cignetti, M., Guenzi, D., Ardizzone, F., Allasia, P., and Giordan, D. (2019). An open-source web platform to share multisource, multisensor geospatial data and measurements of ground deformation in mountain areas. *ISPRS International Journal of Geo-Information*, 9(1):4, doi:10.3390/ijgi9010004.
- Cruz, O. G. D., Mendoza, C. A., and Lopez, K. D. (2021). International roughness index as road performance indicator: A literature review. In *IOP conference series: earth and environmental science*, volume 822, page 012016. IOP Publishing, doi:10.1088/1755-1315/822/1/012016.
- Di Graziano, A., Marchetta, V., and Cafiso, S. (2020). Structural health monitoring of asphalt pavements using smart sensor networks: A comprehensive review. *Journal of Traffic and Transportation Engineering (English Edition)*, 7(5):639–651, doi:10.1016/j.jtte.2020.08.001.
- Elnabwy, M. T., Kaloop, M. R., and Elbeltagi, E. (2013). Talkha steel highway bridge monitoring and movement identification using RTK-GPS technique. *Measurement*, 46(10):4282–4292, doi:10.1016/j.measurement.2013.08.014.
- Golov, E., Evtyukov, S., Protsuto, M., Evtyukov, S., and Sorokina, E. (2022). Influence of the road surface roughness (according to the International Roughness Index) on road safety. *Transportation research procedia*, 63:999–1006, doi:10.1016/j.trpro.2022.06.099.
- Gorda, O. (2020). Topology of information space in construction. *Building production*, 2(70):39–44. (original in Ukrainian).
- Guan, H., Li, J., Cao, S., and Yu, Y. (2016). Use of mobile LiDAR in road information inventory: A review. *International Journal of Image and Data Fusion*, 7(3):219–242, doi:10.1080/19479832.2016.1188860.
- Han, C., Han, T., Ma, T., Tong, Z., and Wang, S. (2023). A BIM-based framework for road construction quality control and quality assurance. *International Journal of Pavement Engineering*, 24(1):2209903, doi:10.1080/10298436.2023.2209903.
- Han, D., Lee, S. B., Song, M., and Cho, J. S. (2021). Change detection in unmanned aerial vehicle images for progress monitoring of road construction. *Buildings*, 11(4):150, doi:10.3390/buildings11040150.
- Hryhorovskiyi, P., Gorda, O., and Chukanova, N. (2020). Information environments in construction. *Building production*, 2:15–19, doi:10.36750/2524-2555.68. (original in Ukrainian).
- Karan, E. P., Sivakumar, R., Irizarry, J., and Guhathakurta, S. (2014). Digital modeling of construction site terrain using remotely sensed data and geographic information systems analyses. *Journal of construction engineering and management*, 140(3):04013067, doi:10.1061/(ASCE)CO.1943-7862.0000822.
- Katkalo, Y. (2012). Determination of actual radii on curves of motorways by electronic tacheometer. *Bulletin of the Belarusian-Russian University*, 3(36):89–95. (original in Russian).
- Kovrov, A. (2022). About the ways to improve the accuracy of mobile laser scanning results. *Vestnik of North-Eastern Federal University. Series "Earth Sciences"*, (1(25)):10–18, doi:10.25587/svf.2022.25.1.009.
- Kuzmin, Y. O. (2019). Recent geodynamics: from crustal movements to monitoring critical objects. *Izvestiya, Physics of the Solid Earth*, 55:65–86, doi:10.1134/S106935131901004X.
- Lobatskaya, R. and Strelchenko, I. (2016). GIS-based analysis of fault patterns in urban areas: A case study of Irkutsk city, Russia. *Geoscience Frontiers*, 7(2):287–294, doi:10.1016/j.gsf.2015.07.004.
- Mill, T., Ellmann, A., Kiisa, M., Idnurm, J., Idnurm, S., Horemuz, M., and Aavik, A. (2015). Geodetic monitoring of bridge deformations occurring during static load testing. *The Baltic Journal of Road and Bridge Engineering*, 10(1):17–27, doi:10.3846/bjrbe.2015.03.
- Můčka, P. (2017). International Roughness Index specifications around the world. *Road materials and pavement design*, 18(4):929–965, doi:10.1080/14680629.2016.1197144.
- Muñoz-Salinas, E., Renschler, C., and Palacios, D. (2009). A GIS-based method to determine the volume of lahars: Popocatepetl volcano, Mexico. *Geomorphology*, 111(1–2):61–69, doi:10.1016/j.geomorph.2008.09.028.
- Nikitin, A. (2018). Determination of motor roads geometry parameters with GNSS receivers. In *Transport of the Asia-Pacific Region*, 2(15):16–17. (original in Russian).
- Pomortseva, O., Kobzan, S., Yevdokimov, A., and Kukhar, M. (2020). Use of geoinformation systems in environmental monitoring. In *The International Conference on Sustainable Futures: Environmental, Technological, Social and Economic Matters (ICSF 2020), E3S Web of Conferences*, volume 166, page 01002. EDP Sciences, doi:10.1051/e3sconf/202016601002.
- Prokhorov, A. and Medvedev, A. (2022). Operational mapping of moving objects using the ICARUS satellite telemetry system. *Geodesy and Cartography*, 987(9):47–56, doi:10.22389/0016-7126-2022-987-9-47-56.
- Ranyal, E., Sadhu, A., and Jain, K. (2022). Road condition monitoring using smart sensing and artificial intelligence: A review. *Sensors*, 22(8):3044, doi:10.3390/s22083044.
- Raza, S., Al-Kaisy, A., Teixeira, R., and Meyer, B. (2022). The role of GNSS-RTN in transportation applications. *Encyclopedia*, 2(3):83, doi:10.3390/encyclopedia2030083.
- Samsonov, S. and Baryakh, A. (2020). Estimation of deformation intensity above a flooded potash mine near Berezniki (Perm Krai, Russia) with SAR interferometry. *Remote Sensing*, 12(19):3215, doi:10.3390/rs12193215.
- Scalco, L., Bordin, F., de Souza, E. M., Brum, D., Racolte, G., Mar-

- ques Jr, A., da Silveira Jr, L. G., and Veronez, M. R. (2023). Improving geometric road design through a virtual reality visualization technique. *TRANSPORTES*, 31(1):e2838–e2838, [doi:10.58922/transportes.v31i1.2838](https://doi.org/10.58922/transportes.v31i1.2838).
- Shutin, M. D. and Dolgov, D. V. (2019). Creating a digital passport of the object during the survey of transport infrastructure. In *2019 IEEE Conference of Russian Young Researchers in Electrical and Electronic Engineering (EIConRus)*, pages 1485–1487. IEEE, [doi:10.1109/EIConRus.2019.8657299](https://doi.org/10.1109/EIConRus.2019.8657299).
- Taşçi, L. (2015). Deformation monitoring in steel arch bridges through close-range photogrammetry and the finite element method. *Experimental techniques*, 39:3–10, [doi:10.1111/ext.12022](https://doi.org/10.1111/ext.12022).
- Tikhomirov, P. V., Skrypnykov, A. V., A, V. I., Kazachek, M. N., Zelikov, V. A., and Bondarev, A. B. (2022). Information-intelligent system for improving geometric control of the construction of road rounds. *Izvestiya SPbLTA*, (239):161–171, [doi:10.21266/2079-4304.2022.239.161-171](https://doi.org/10.21266/2079-4304.2022.239.161-171).
- Vatseva, R., Solakov, D., Tcherkezova, E., Simeonova, S., and Trifonova, P. (2013). Applying GIS in seismic hazard assessment and data integration for disaster management. *Intelligent Systems for Crisis Management: Geo-information for Disaster Management (Gi4DM) 2012*, pages 171–183, [doi:0.1007/978-3-642-33218-0_13](https://doi.org/10.1007/978-3-642-33218-0_13).